



Numerical and Experimental Analysis of Perforated Plate for Ultra Micro Gas Turbine Combustion Chamber

Muhamad Maris Al Gifari^{1,2,*}, Firman Hartono³, Prihadi Setyo Darmanto⁴, Iman Kartolaksono Reksowardojo⁵, Yohanes Bimo Dwianto³

- ¹ Automotive Engineering Education Study Program, Faculty of Technology and Vocational Education, Universitas Pendidikan Indonesia, Bandung, Indonesia
- ² Aerospace Engineering Doctoral Program, FacultyMO of Mechanical and Aerospace Engineering, Institut Teknologi Bandung, Jalan Ganesa 10, Bandung, Indonesia
- ³ Fluid Dynamics and Propulsion Research Group, Faculty of Mechanical and Aerospace Engineering, Institut Teknologi Bandung, Jalan Ganesa 10, Bandung, Indonesia
- ⁴ Thermal Science and Engineering Research Group, Faculty of Mechanical and Aerospace Engineering, Institut Teknologi Bandung, Jalan Ganesa 10, Bandung, Indonesia
- ⁵ Mechanical Engineering Study Program, Pertamina University, Teuku Nyak Arief, Jakarta Selatan, DKI Jakarta, Indonesia

ARTICLE INFO

Article history:

Received 17 October 2024

Received in revised form 19 November 2024

Accepted 21 December 2024

Available online 31 January 2025

Keywords:

Ultra micro gas turbine; combustion chamber; porous media; perforated plate; flow characteristic

ABSTRACT

The role of ultra-micro gas turbines becomes increasingly strategic in the global shift towards electrification. Currently, battery density significantly lags behind kerosene, making hybrid technology, particularly involving ultra-micro gas turbines, a pertinent solution. Development challenges primarily revolve around engine components operating at high speeds of up to 2 million rpm. The use of porous media, while effective, is limited in Indonesia, prompting the exploration of alternatives. The perforated plate emerges as a promising solution, capable of inducing turbulence and streamlining flow. This study evaluates the flow patterns of the perforated plate, focusing on turbulence generation and combustion stability. Results indicate the potential of the perforated plate to replace porous media with lower pressure loss. The combination of the perforated plate produces the highest-pressure loss, increasing with Reynolds number, significantly contributing to combustion stability. The single perforated plate staggered scheme shows promising characteristics because its flow structure generates high turbulence intensity with low pressure loss, demonstrating practical applicability potential on a larger scale.

1. Introduction

The micro gas turbine holds a strategic value in addressing future energy demands, especially as a tool that convert mechanical work to electricity [1]. Its exceptional capability to produce high power output within a compact size renders it versatile for various applications [2,3]. Its adaptable nature for integration into portable devices and integrated systems has positioned it as a significant research focus [3], including the development of hybrid systems [4-6]. The emergence of hybrid systems is

* Corresponding author.

E-mail address: author.mail@gmail.com (Muhamad Maris Al Gifari)

propelled by the fact that the energy density of kerosene currently exceeds that of lithium-ion batteries by a factor of 45 [6,7], necessitating combustion engines to bolster system efficiency. The limited energy density of batteries further imposes restrictions on their applications, thereby elevating the promise of micro gas turbines. Another pivotal aspect of micro gas turbine development is its fuel flexibility [8-10], including a gas predominantly derived from waste [11]. It is within this context that the strategic value of micro gas turbines becomes evident, accentuating the urgency for their advancement.

The development of ultra-micro gas turbines has been carried out by various institutions, such as MIT and the Korea Institute of Machinery and Materials. In general, the challenges faced are manufacturing issues related to rotor dynamics at rotational speeds ranging from 400 to 2000 krpm[4]. Nevertheless, the development of ultra-micro gas turbines can still be pursued by commencing from the combustion chamber as a non-rotating component. The challenges faced in the design and development of ultra-micro gas turbine combustion chambers include maintaining flame stability with low pressure drop [12] and low combustion efficiency [13]. This issue is addressed through the implementation of porous media in the combustion chamber because porous media can generate turbulence [14] and optimize heat utilization by raising the reactant temperature using heat from the combustion zone through conduction and radiation mechanisms [12,13,15]. In his 2017 study, Turkeli [12] utilized porous media in the ultra-micro gas turbine combustion chamber fuelled by liquid LPG. The results demonstrated enhanced combustion stability, efficiency, and a significant reduction in pollutants. In his 2021 study, Lukas Badum [4] proposed the utilization of porous media in the design of ultra-micro gas turbines for the combustion chamber. This recommendation is based on the advantages of high energy density, a favourable turn-down ratio, and stable combustion. Furthermore, Mohaddes conducted an investigation on the impact of porous media application in the Brayton gas turbine cycle [16], concluding that porous media can significantly enhance the thermal efficiency of the Brayton cycle in gas turbine engines. This improvement stems from the more efficient and stable combustion occurring within the high thermal inertia porous medium. Additionally, the implementation of porous media combustion can lead to a reduction in NO_x and CO emissions in gas turbine engines [16]. It is evident how porous media can offer solutions to the challenges encountered in ultra-micro gas turbine combustion chambers.

Porous media manufacturing is a relatively recent development that has been typically outsourced outside of Indonesia due to the critical consideration of porosity and its direct impact on performance, as substantiated by existing research [15]. An alternative approach emerges in the form of perforated plates, which not only promote turbulence generation [17], but also have a physical capacity to facilitate heat conduction from the combustion zone to the reactant flow region. Additionally, perforated plates offer advantages in terms of ease of production, making them a feasible choice for Indonesia as a developing nation. Research focused on the formation of perforated plates for gas turbine applications is essential to strike a balance between achieving adequate turbulence and minimizing pressure drop. Turbulence significantly influences combustion stability like swirler effect that can enhanced combustion [18], and maintaining control over pressure drop within the combustion chamber is paramount to the overall performance of ultra-micro gas turbines.

Previous research has utilized perforated plates for various applications. Perforated plates have been employed to generate turbulence intensity as demonstrated by Liu *et al.*, [19]. Perforated plates are utilized for stabilizing combustion by employing two perforated plates, where the stability effect is observed through flame visualization and compared with experiments [20]. Research on perforated plates highlights how their vertical placement induces permeability and turbulence effects, conducted by Shahzad *et al.*, [21] with these effects observed through DNS simulations. Perforated plates are also utilized to mitigate acoustic modes in combustion, a study conducted by Zhou *et al.*,

[22], and Gullaoud and Nicoud [23]. The utilization of perforated plates for combustion stability and performance enhancement is numerically, and experimentally investigated in a biomass-burning reactor by Erdiwansyah *et al.*, [24,25]. Flow observations on single perforated plates are also conducted, where the primary aim is to minimize swirl [26], then observations on double perforated plates are also employed with a formation of two perforated plates, where pressure loss is a major parameter, conducted by La Rosa *et al.*, [27] experimentally, and detailed discussions with numerical simulations [28]. Multistage observations are also utilized in studying propane-air mixture propagation to accelerate propagation speed or flame speed [29].



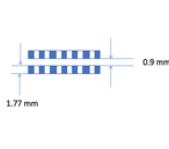
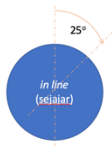
This study aims to investigate the formation of perforated plates and its correlation with pressure reduction as a constraint within the context of ultra-micro gas turbines featuring a 5 cm burner diameter. By doing so, this research introduces an alternative porous media material, where perforated plates offer cost-effective manufacturing and precise flow analysis.

2. Methodology

2.1 Experimental Scheme for Validating CFD Simulation Results

The experiments were conducted with the aim of determining the pressure losses for five structured porous media models subjected to five different air mass flow rates. Each structured porous media (perforated plate) pattern was tested with varying mass flow rates, contingent upon the resistance exerted by the perforated plate and limited by the capacity of the employed blower. Five distinct data points were collected for each perforated plate pattern, which were considered representative enough for validation purposes. The tested structured porous media model can be seen in Table 1.

Table 1
 The profiles of the structured porous media to be tested

Pattern				
Scheme Number	1	2	3	4
Thickness(mm)	2.76	2.76	1.77	1.77
n	62	70	62	62
FAR	0.13	0.15	0.13	0.13
Configuration	SPP	SPP	DPP	DPP

All patterns of structured porous media have hole diameters of 2 mm, representing the manufacturing capability currently available in the Indonesian region. These structured porous media are manufactured with a diameter of 44 mm. In Table 1, the term FAR is defined as the ratio between the hole area and the total surface area of the structured porous media. The symbol 'n' represents the number of holes of the structured porous media. There are two configurations of structured porous media: the first one is Single Perforated Plate (SPP), and the second one is Double Perforated Plate (DPP). These configurations are listed in Table 1 as numbers 3 and 4. Configuration DPP in number 3 of Table 1 uses perforated plates with holes in the same position, while number 4 represents the same configuration as number 3, but with the downstream of structured porous media rotated 25 degrees. The use of double configurations of perforated plates aims to observe the influence of increased pressure loss resulting from the addition of perforated plates on turbulence production. The experimental results will be compared with the pressure loss of regular porous

media, specifically types sintered stainless steel R200, as shown in Figure 1, with a thickness of 2.76 mm. The structured and regular porous medias were stored in the testing chamber following the scheme illustrated in Figure 2.

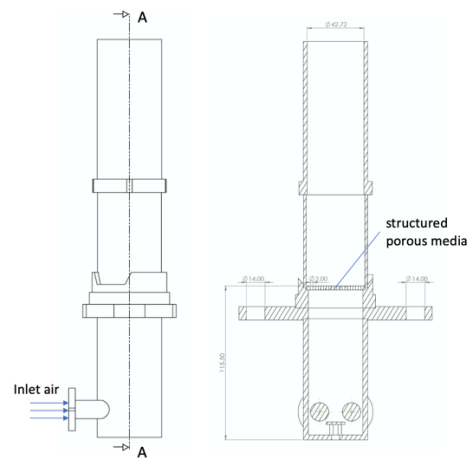
The testing scheme for measuring pressure loss of the porous medias is depicted in Figure 3. The experiment is cold flow. The essence of this scheme is to provide air flow using a blower, measuring air mass flow rate, and measuring pressure before passing through porous media using a transducer.



Fig. 1. Sintered stainless steel Porous Media R200



(a)



(b)

Fig. 2. (a) Experiment section test (b) Cutting draw

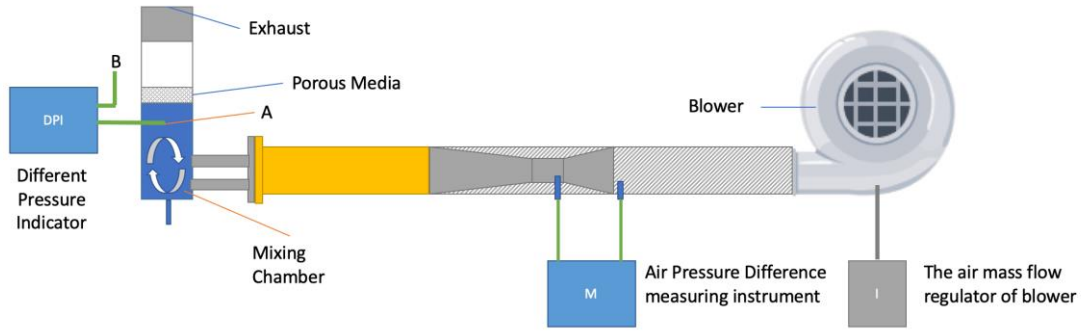


Fig. 3. Cold flow experiment scheme

The blower utilized in the study had a power rating of 1.5 kilowatts and was controlled by an inverter to vary the mass flow rate flowing into the porous media. Air mass flow rate measurements were conducted using the mass flow rate equation (Eq. (1)). The velocity was measured using a venturi tube, and the pressure difference in the venturi was measured using a Betz micromanometer.

$$\dot{m} = \rho Av \quad (1)$$

In Eq. (1), the mass flow rate is denoted by \dot{m} , where ρ represents the density, A is the cross-sectional area, and v is the air flow velocity. Subsequently, the pressure difference between the upstream and downstream of the porous media was measured using a DPI (different pressure indicator). Upstream pressure is measured at point A (before the porous media) and downstream the ambient pressure represents downstream pressure. This pressure difference describes the pressure loss after passing through a porous medium [30]. The DPI specifications outlined in Table 2.

Table 2

DPI specification	
Range	0.25 to 200 in.H ₂ O (62.21 to 49768 Pa)
Compensated temperature range	20°F to 120°F (-7 to 49oC)
Temperature effect	0.004% per °F above the compensated range
Repeatability	0.01% of span (range 0/1 in.H ₂ O or higher) 0.02% of span (range under 1.0 in.H ₂ O)
Sensitivity	0.002% of span
Under/Over pressure capability	-15 to 50 psi

The specifications data mentioned in Table 2 were used to calculate the uncertainty of the DPI measurements. Measurement uncertainty was assessed using Eq. (2).

$$u_d = \sqrt{u_0^2 + \sum_{i=1}^{n_I} u_{I_i}^2} \quad (2)$$

The DPI uncertainty (u_d) is a function of both zero uncertainty and the sum of all elemental instrumentation uncertainties. The zero uncertainty (u_0) itself is half the resolution of the DPI device. Instrumentation uncertainty (u_I) is the sum of elemental errors, where in this case, the elemental errors include repeatability error (\tilde{e}_r) and sensitivity error (\tilde{e}_s), as described in Eq. (3)."

$$u_I = FSO \cdot \sqrt{\tilde{e}_R^2 + \tilde{e}_S^2} \quad (3)$$

$$\tilde{e}_R = \frac{2S_x}{FSO} \quad (4)$$

$$\tilde{e}_S = \frac{e_{K,max}}{FSO} \quad (5)$$

The repeatability error and sensitivity are defined by Eq. (4) and Eq. (5), where FSO (Full Scale Output Maximum) represents the highest-pressure measurement value achievable by the DPI, specifically 200 inch. H₂O or equivalent to 49,768 Pa. The symbol S_x defined here indicates sensitivity, and the span in this specification is the highest value minus the lowest value detectable by the DPI. In this case, the minimum is 0.25 inch.H₂O. Sensitivity in the specification data is defined as $e_{K,max}$ in Eq. (5). The measurement uncertainty (u_d) of this DPI, based on the specifications outlined in Table 1 and Eq. (2) to Eq. (5), is 10 Pa.

2.2 Computational Fluid Dynamics Simulation Scheme for Experimental Results Validation

The first thing to be considered in CFD simulation of the flow around a perforated plate is the number of cells. The parameter targeted in this simulation is pressure loss, so the magnitude of the pressure loss generated by the simulation must be independent of the grid count. The grid count was selected by an independent grid test. The second aspect that important in CFD simulation is the turbulence model. The turbulence model utilized should represent the existing phenomena. The choice of the turbulence model is based on the observed phenomena and is reinforced by research conducted by others.

The results of the grid independence test can be observed in Figure 4, demonstrating that the grid count does not affect the magnitude of the pressure loss. Based on Figure 4, the number of cells taken as the standard to ensure independence from the cell count is more than 881,900 cells for a single perforated plate and 851.880 cells for the double perforated plate scheme (based on Figure 4). The results of the 3D model meshing process can be seen in Figure 5 for SPP and DPP scheme.

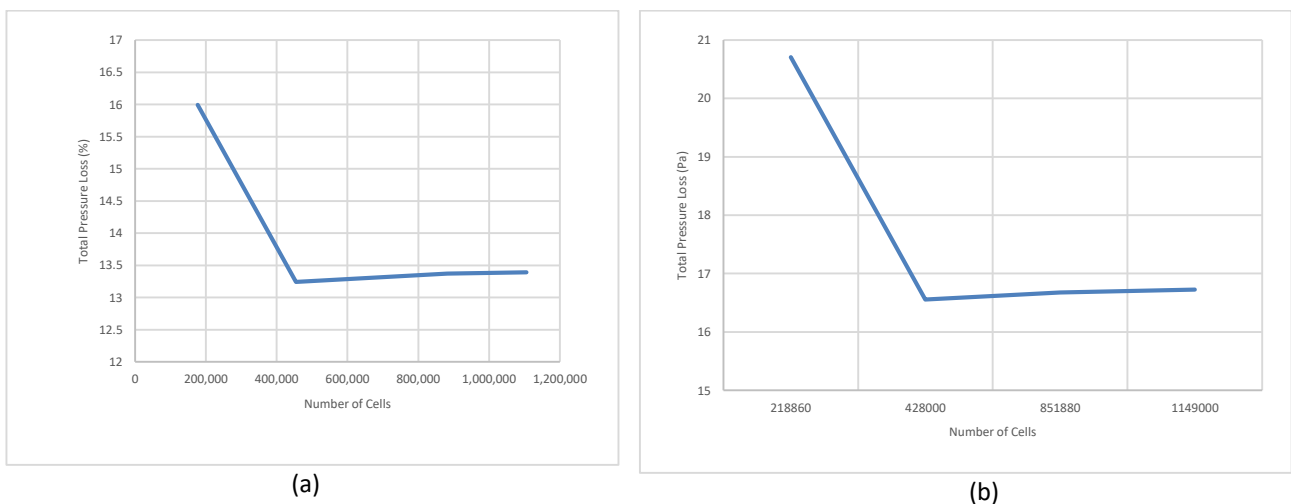


Fig. 4. Result of Grid Independence Test for (a) SPP and (b) DPP

The choice of the turbulence model for this simulation is based on considerations of near-wall phenomena and the dominant occurrence of separation [17]. The turbulence model that fits this phenomenon is k-omega SST. The material utilized in this simulation is air with a constant density 1.225 kg/m³ and viscosity 1.7894x10⁻⁵ kg/(m.s). The convergence criterion applied in the analysis is set at 10⁻⁷.

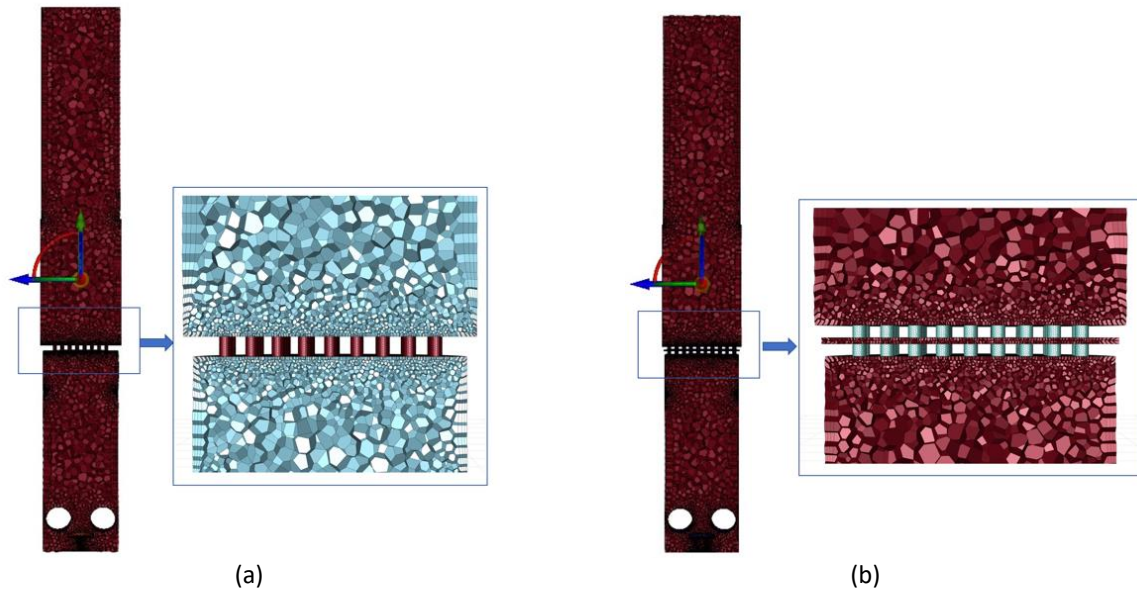


Fig. 5. Meshing structure of (a) single perforated plate (b) double perforated plate

The boundary conditions at the inlet comprise a mass flow inlet with a turbulent intensity of 5% and a turbulent viscosity ratio of 10. The mass flow inlet applied for each scheme depends on experimental outcomes; Table 3 illustrates five mass flow rates for each scheme.

Table 3

Sets the mass flow for each scheme

Massflow (g/s)			
Scheme 1 SPP	Scheme 2 SPP	Scheme 3 DPP	Scheme 4 DPP
0.77	1	0.7	0.754
1.2	1.5	1.13	1.156
1.6	2	1.56	1.556
2	2.52	1.97	1.966
2.4	3	2.38	2.363

In addition to simulating the scenarios that will be validated based on experiments, this CFD simulation was also conducted to explore and understand how the patterns of structured porous media (perforated plate) geometry can replace regular porous media by considering pressure loss and turbulent intensity as parameters. Variations were made by combining structured porous media with a thickness of 1.77 mm, ranging from 1 to 3 layers of perforated plates, along with the spacing between the perforated plates.

3. Result

The CFD results obtained using the k-omega SST turbulence model and experiments for all patterns exhibit consistency, wherein the CFD results are consistently greater than the experimental results, as indicated in all Figure 6. The pressure loss difference increases with the rise in mass flow rates, and this phenomenon applies not only to Single Perforated Plates (SPP) but also to Double Perforated Plates (DPP).

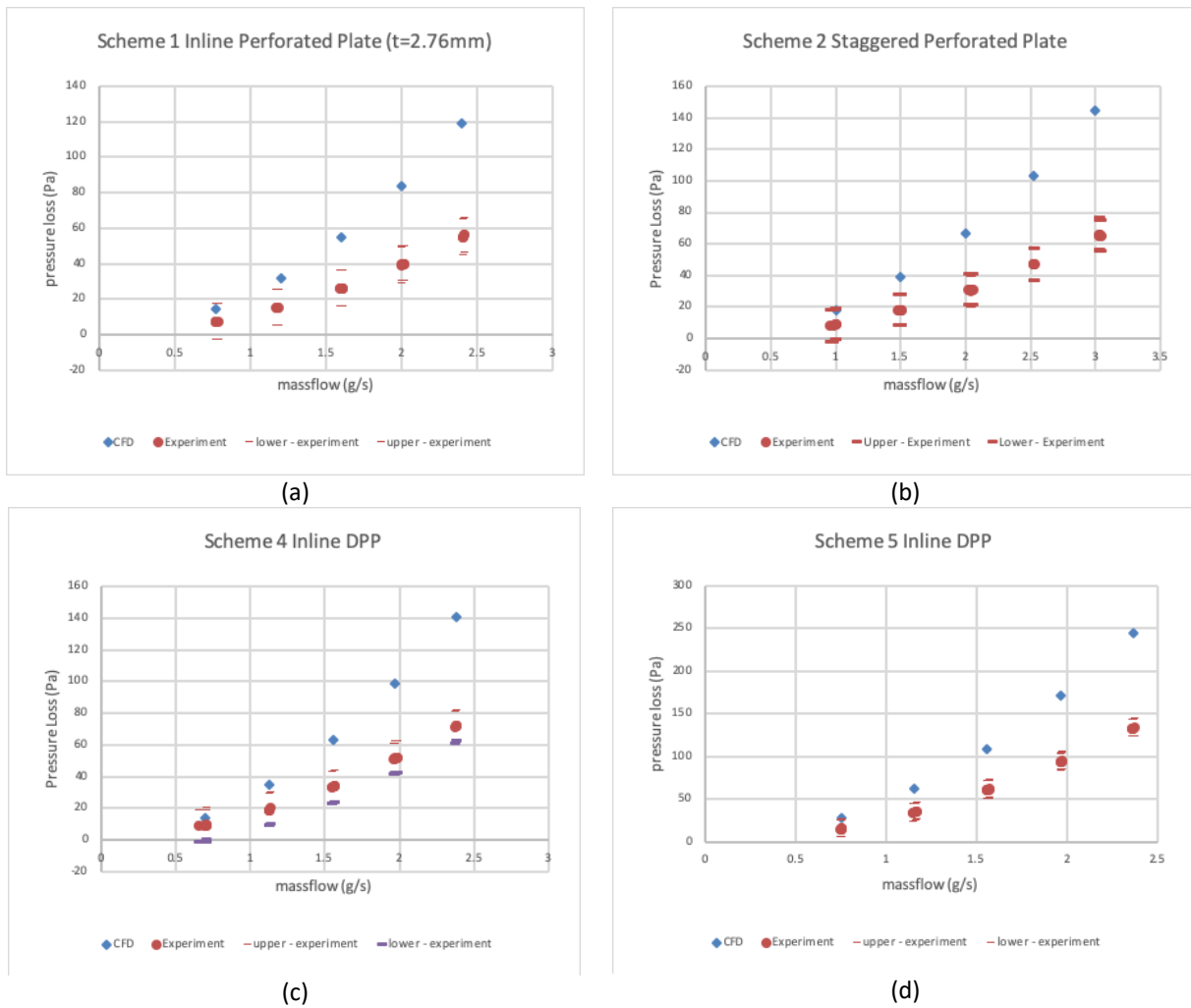


Fig. 6. Pressure loss v massflow of each scheme for CFD and experiment results

Figure 6 illustrates the consistency where the pressure loss results from CFD are greater than the experimental results. The experimental results and CFD simulations of all schemes are similar, namely the CFD results are greater than the experimental results. To assess the consistency of the outcomes, a comparison is made between the schemes in terms of both CFD and experimental data. The patterns between experiments and CFD are also consistent, meaning each pattern has the same sequence for its pressure loss values, as shown in Figure 7. The Double Perforated Plate (DPP) pattern for scheme 5 has the highest-pressure loss for both CFD and experiments, while the staggered Single Perforated Plate (SPP) pattern has the smallest pressure loss. If we observe the pressure loss, as indicated by both CFD simulations and experiments, both can be approximated by a quadratic relationship with respect to mass flow rates.

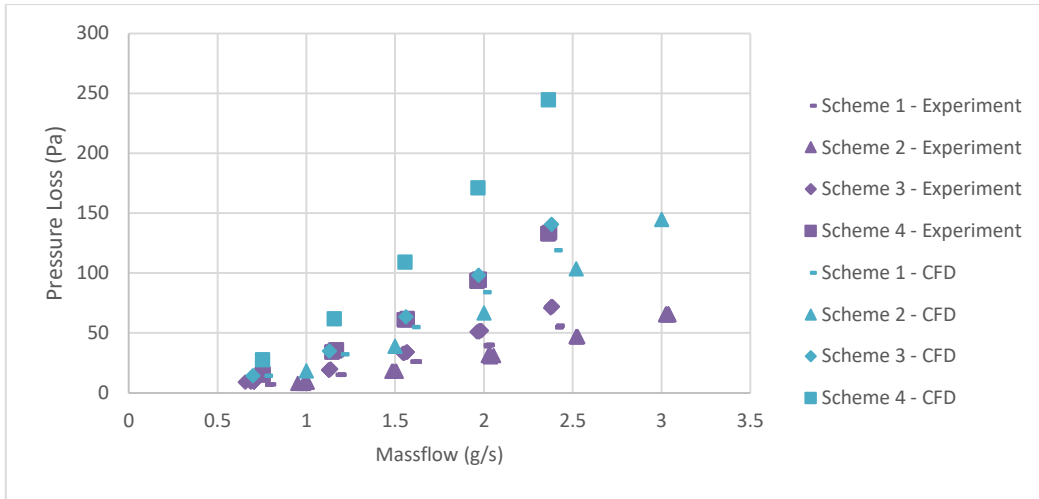


Fig. 7. Comparison of pressure loss for CFD and experiment for each scheme

The relationship between speed and pressure loss is quadratic [31], and mass flow is directly proportional to speed. This is in line with the results of experiments and CFD simulations that have been carried out. This relationship can also be further explored by presenting the data in non-dimensional form, namely the hole diameter-based Reynolds number (Re_0) defined in Eq. (6), and the Euler number $\left(\frac{\Delta p}{\rho U_0^2}\right) Re_0$, where $\Delta p, \rho, U_0$ are pressure loss, air density, and mean velocity through perforated plate hole respectively. The relationship between these two-dimensional numbers is described in Eq. (7) where α, β are constant [31]. The symbols ρ, μ represent the density and viscosity of air respectively. Eq. (7) can also be a tool for determine the occurrence of turbulence.

$$Re_0 = \frac{\rho U_0 D_0}{\mu} \tag{6}$$

$$\left(\frac{\Delta p}{\rho U_0^2}\right) Re_0 = \alpha + \beta Re_0 \tag{7}$$

Figure 8 shows the experimental data when presented in the form of defined Euler numbers and Reynolds numbers.

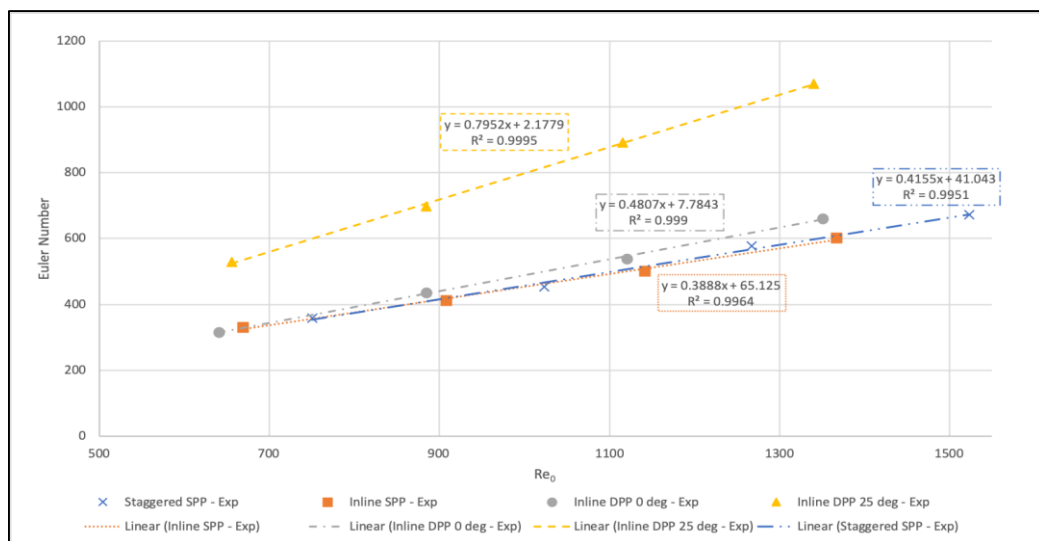


Fig. 8. Euler Number v Re_0 for experiment results for all scheme

All experimental results carried out can be said to be correct because the relationship between the Euler number and Re_0 is linear. Then, if you take α and β values and summarize them in table 4. Perforated plate with double scheme with scheme 4 (Inline DPP 25 deg) has the largest beta value, which means that every increase in the hole Reynolds number will be followed by a greater increase in pressure loss compared to the others. This corresponds to the natural conditions under which this scheme produces the greatest pressure loss.

Table 4
 Values of α dan β for every scheme

Scheme	Porosity (φ)	Beta (β)	Alfa (α)
Inline SPP	14%	0.3888	65.125
Staggered SPP	15%	0.4155	41.043
Inline DPP 0 deg	14%	0.4807	7.7843
Inline DPP 25 deg	14%	0.7952	2.1779

Furthermore, the results of this experiment are used to compare the pressure loss that occurs in a perforated plate with a porous media. The porous media applied in this research is sintered stainless steel R200 with a porosity level of 49-54%. This comparison was carried out to investigate the potential of perforated plates in terms of pressure loss. The focus of the comparison is focused on the perforated plate pattern with a double inline scheme which has undergone a rotation of 25 degrees. This rotation is significant because the scheme shows the highest-pressure loss compared to other schemes. Thus, a comparison between the pattern of the perforated plate in the rotation scheme and the sintered porous medium of R200 stainless steel can be found in detail in Figure 9.

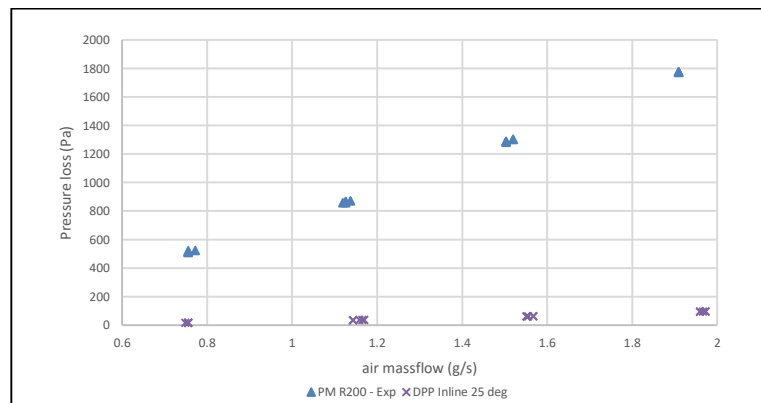


Fig. 9. Differences in pressure loss values between sintered stainless steel R200 porous media and DPP-inline 25 schemes

The pressure loss values of the sintered stainless steel porous media are significantly greater compared to the DPP-inline 25 scheme, and they increase further with the higher mass flow rates. It is evident from this observation how the perforated plate demonstrates a potential for lower pressure loss.

Seeing the potential for small pressure loss, now how the perforated plate produces turbulent flow. When the combustion chamber is only a shell tube without a perforated plate, the Reynolds number is 547 with a diameter of 44 mm as a reference for the highest mass flow, namely 1.9 g/s, then the category is laminar [31]. When a perforated plate is employed, its presence induces turbulent flow. Turbulent flow is advantageous for combustion chambers [32]. Stability can be

achieved at lower speeds and equivalence ratio values [33]. When the Euler number and Re_0 plot exhibits a slope, as illustrated in Figure 8, it signifies that the flow has transitioned to turbulence [31].

The next aspect to be observed is the turbulent intensity, aiming to understand how the perforated plate transforms the flow into turbulence. The point of interest here is whether generating turbulent intensity requires high pressure loss. The development of turbulent intensity for each scheme is presented in Figure 10, with data representation utilizing non-dimensional parameters, namely the distance from the perforated plate divided by the hole diameter [19].

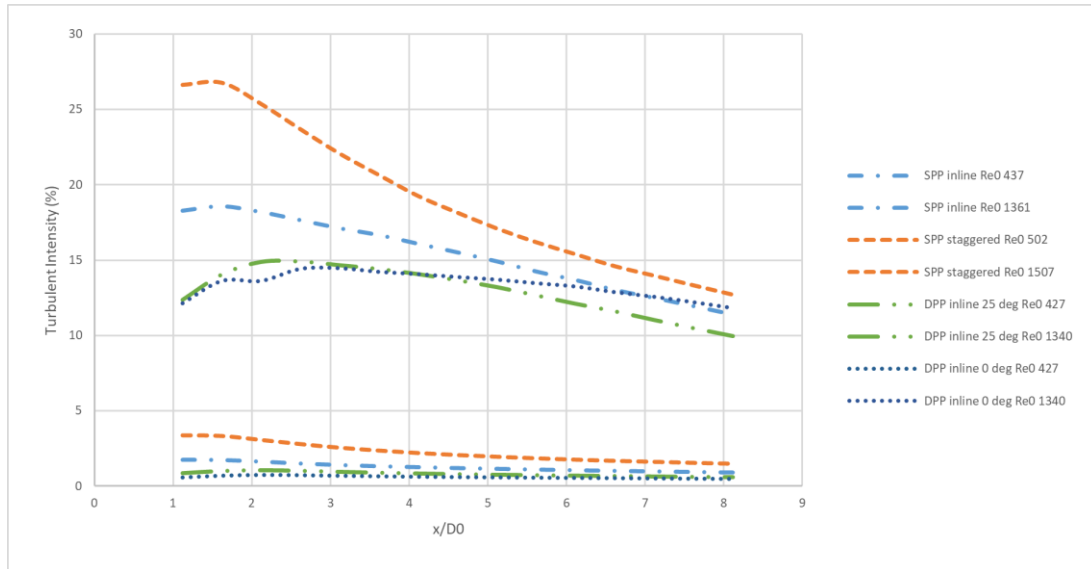


Fig. 10. Development of turbulent intensity in downstream of the perforated plate

It can be seen from Figure 10 that the pressure loss is not proportional to the intensity formed. The perforated plate scheme with a staggered single perforated plate pattern has the highest turbulent intensity. This shows that the staggered pattern produces better turbulent intensity than the inline pattern, even though the resulting pressure loss is small.

Next, based on the simulation results of turbulent intensity plots, it is essential to scrutinize the flow structure in more detail, particularly in two cases: staggered, which exhibits high turbulent intensity, and the scheme of a double perforated plate rotated by 25 degrees. The first aspect to be observed is the flow pattern depicted by velocity vectors.

Figure 11 depicts the velocity vectors in each scheme for the highest hole Reynolds number Re_0 , 1507 for SPP staggered and 1340 for DPP inline 25 deg. In this region, there is a recirculation zone and a potential core or jet area [34]. This recirculation zone subsequently becomes a fundamental consideration to support stability in the ultra-micro gas turbine combustion chamber [35].

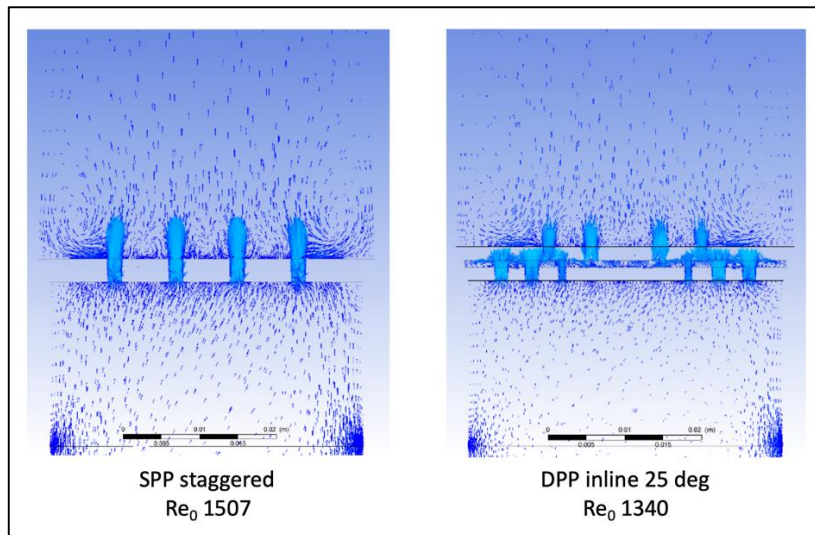


Fig. 11. Development of turbulent intensity in downstream of the perforated plate

4. Conclusions

Perforated plates have the potential to replace porous media by offering much smaller pressure losses with a much smaller rate of increase as the air mass flow rate increases. This shows that the combination of perforated plates has the potential to replace porous media in creating combustion stability.

The combination of perforated plates produces the highest pressure loss with a slope level of 0.7952, meaning that for every increase in the Reynolds number, the resulting pressure loss is 0.7952 Pa. The single perforated plate staggered scheme has a slope of 0.4155, the flow structure in the perforated plate actually produces large turbulent intensity with small pressure loss based on CFD simulations with different levels of pressure loss compared to experiments of 79 Pa at Re_0 1507 with experimental results.

The subsequent research will be conducted using combustion methods to examine the intensity of turbulence, with a specific focus on combustion quality and stability. The study will employ two primary approaches: experimental analysis to observe phenomena empirically and Computational Fluid Dynamics (CFD) simulations to analyze how flow structures influence combustion stability. The findings from this research will serve as a foundation for designing the implementation of a perforated plate in the combustion chamber of an ultra-micro gas turbine.

Acknowledgement

This work is supported by Research, Community Services, and Innovation Program (PPMI) ITB 2023. I will appreciate Laurentius Laksamana Putra Samudera, Rizal Gidion Solissa, Adi Suryabudi Wibawa, Firas Altair Zuhair and Kenneth Christian (Institut Teknologi Bandung) for all expertise assistance and technical contributions on the research projects.

References

- [1] Salleh, Hamidon, Bukhari Manshoor, Izzuddin Zaman, Shahrin Hisham Amirnordin, Amirul Asyraf, Amir Khalid, Syabillah Sulaiman, and Wahid Razzaly. "Effects of fluid flow characteristics and heat transfer of integrated impingement cooling structure for micro gas turbine." *CFD Letters* 12, no. 9 (2020): 104-115. <https://doi.org/10.37934/cfdl.12.9.104115>

- [2] Capata, Roberto. "Ultra Micro Gas Turbines." *Efficiency, Performance and Robustness of Gas Turbines* (2012): 5. <https://doi.org/10.5772/37829>
- [3] Nagashima, Toshio. "Lessons learnt from ultra-micro-gas turbine development at University of Tokyo." *Invited Lecture, von Karman Institute for Fluid Dynamics Lecture Series on Micro Gas Turbines, Bursseis* (2005).
- [4] Janovec, Michal, Jozef Čerňan, Filip Škultéty, and Andrej Novák. "Design of batteries for a hybrid propulsion system of a training aircraft." *Energies* 15, no. 1 (2021): 49. <https://doi.org/10.3390/en15010049>
- [5] Schneider, Michael, Jens Dickhoff, Karsten Kusterer, Wilfried Visser, Eike Stumpf, Jan-Philipp Hofmann, and Dieter Bohn. "Development of a gas turbine concept for electric power generation in a commercial hybrid electric aircraft." In *Turbo Expo: Power for Land, Sea, and Air*, vol. 58547, p. V001T01A028. American Society of Mechanical Engineers, 2019. <https://doi.org/10.1115/GT2019-92065>
- [6] Badum, Lukas, Boris Leizeronok, and Beni Kukurel. "New Insights From Conceptual Design of an Additive Manufactured 300 W Microgas Turbine Toward Unmanned Aerial Vehicle Applications." *Journal of Engineering for Gas Turbines and Power* 143, no. 2 (2021): 021006. <https://doi.org/10.1115/1.4048695>
- [7] Löbbberding, Hendrik, Saskia Wessel, Christian Offermanns, Mario Kehrer, Johannes Rother, Heiner Heimes, and Achim Kampker. "From cell to battery system in BEVs: Analysis of system packing efficiency and cell types." *World Electric Vehicle Journal* 11, no. 4 (2020): 77. <https://doi.org/10.3390/wevj11040077>
- [8] De Vries, J., and E. L. Petersen. "Autoignition of methane-based fuel blends under gas turbine conditions." *Proceedings of the combustion institute* 31, no. 2 (2007): 3163-3171. <https://doi.org/10.1016/j.proci.2006.07.206>
- [9] Valera-Medina, Agustin, Steven Morris, Jon Runyon, Daniel G. Pugh, Richard Marsh, Paul Beasley, and Thomas Hughes. "Ammonia, methane and hydrogen for gas turbines." *Energy Procedia* 75 (2015): 118-123. <https://doi.org/10.1016/j.egypro.2015.07.205>
- [10] Huth, Michael, and Andreas Heilos. "Fuel flexibility in gas turbine systems: impact on burner design and performance." In *Modern gas turbine systems*, pp. 635-684. Woodhead Publishing, 2013. <https://doi.org/10.1533/9780857096067.3.635>
- [11] Singh, Chander Kumar, Anand Kumar, and Soumendu Shekhar Roy. "Quantitative analysis of the methane gas emissions from municipal solid waste in India." *Scientific reports* 8, no. 1 (2018): 2913. <https://doi.org/10.1038/s41598-018-21326-9>
- [12] Turkeli-Ramadan, Z., R. N. Sharma, and R. R. Raine. "Experimental study on flat flame combustion for ultra micro gas turbine applications." *Combustion Science and Technology* 189, no. 8 (2017): 1307-1325. <https://doi.org/10.1080/00102202.2017.1294588>
- [13] Jiaqiang, E., Yaqian Mei, Changling Feng, Jiangjun Ding, Lei Cai, and Bo Luo. "A review of enhancing micro combustion to improve energy conversion performance in micro power system." *International Journal of Hydrogen Energy* 47, no. 53 (2022): 22574-22601. <https://doi.org/10.1016/j.ijhydene.2022.05.042>
- [14] Mohamad, A. A. "Combustion in porous media: fundamentals and applications." In *Transport phenomena in porous media III*, pp. 287-304. Pergamon, 2005. <https://doi.org/10.1016/B978-008044490-1/50015-6>
- [15] Wu, Shiguang, Shitu Abubakar, and Yuqiang Li. "Thermal performance improvement of premixed hydrogen/air fueled cylindrical micro-combustor using a preheater-conductor plate." *International Journal of Hydrogen Energy* 46, no. 5 (2021): 4496-4506. <https://doi.org/10.1016/j.ijhydene.2020.10.237>
- [16] Mohaddes, Danyal, Clarence T. Chang, and Matthias Ihme. "Thermodynamic cycle analysis of superadiabatic matrix-stabilized combustion for gas turbine engines." *Energy* 207 (2020): 118171. <https://doi.org/10.1016/j.energy.2020.118171>
- [17] Śmierciew, Kamil, Dariusz Butrymowicz, Jarosław Karwacki, and Jerzy Gagan. "Numerical prediction of homogeneity of gas flow through perforated plates." *Processes* 9, no. 10 (2021): 1770. <https://doi.org/10.3390/pr9101770>
- [18] Samiran, Nor Afzanizam, Khalil Firdaus Bin Abu Mansor, Razlin Abd Rashid, and Muhammad Suhail Sahul Hamid. "CFD Simulation Analysis of Non-Premixed Combustion using a Novel Axial-Radial Combined Swirler for Emission Reduction Enhancement." *CFD Letters* 15, no. 6 (2023): 1-11. <https://doi.org/10.37934/cfdl.15.6.111>
- [19] Liu, Rui, David SK Ting, and Gary W. Rankin. "On the generation of turbulence with a perforated plate." *Experimental thermal and fluid science* 28, no. 4 (2004): 307-316. [https://doi.org/10.1016/S0894-1777\(03\)00106-7](https://doi.org/10.1016/S0894-1777(03)00106-7)
- [20] Rahman, Fitrahtur. "Pengaruh Jarak Antara Perforated Plate Terhadap Kestabilan Api Dan Temperatur Gas Buang Pada Meso-Scale Combustor." PhD diss., Universitas Brawijaya, 2017.
- [21] Shahzad, Haris, Stefan Hickel, and Davide Modesti. "Permeability and turbulence over perforated plates." *Flow, Turbulence and Combustion* 109, no. 4 (2022): 1241-1254. <https://doi.org/10.1007/s10494-022-00337-7>
- [22] Zhou, Hao, Zihua Liu, Hao Fang, Chengfei Tao, Mingxi Zhou, and Liubin Hu. "Attenuation effects of perforated plates with heterogeneously distributed holes on combustion instability in a spray flame combustor." *Journal of Mechanical Science and Technology* 34 (2020): 4865-4875. <https://doi.org/10.1007/s12206-020-1042-2>

- [23] Gullaude, Elsa, and Franck Nicoud. "Effect of perforated plates on the acoustics of annular combustors." *AIAA journal* 50, no. 12 (2012): 2629-2642. <https://doi.org/10.2514/1.J050716>
- [24] Husin, Husni, Asri Gani, and Rizalman Mamat. "Modification of perforated plate in fluidized-bed combustor chamber through computational fluid dynamics simulation." *Results in Engineering* 19 (2023): 101246. <https://doi.org/10.1016/j.rineng.2023.101246>
- [25] Husin, Husni, Asri Gani, and Rizalman Mamat. "Modification of perforated plate in fluidized-bed combustor chamber through computational fluid dynamics simulation." *Results in Engineering* 19 (2023): 101246. <https://doi.org/10.1016/j.rineng.2023.101246>
- [26] Rodrigues, Neil S., Oluwatobi Busari, William CB Senior, Colin T. McDonald, Andrew J. North, YunTao Chen, W. Laster, Scott E. Meyer, and Robert P. Lucht. "The development and performance of a perforated plate burner to produce vitiated flow with negligible swirl under engine-relevant gas turbine conditions." *Review of Scientific Instruments* 90, no. 7 (2019). <https://doi.org/10.1063/1.5100180>
- [27] La Rosa, Davide Maria, Marco Maria Agostino Rossi, Giacomo Ferrarese, and Stefano Malavasi. "On the pressure losses through multistage perforated plates." *Journal of Fluids Engineering* 143, no. 6 (2021): 061205. <https://doi.org/10.1115/1.4049937>
- [28] La Rosa, Davide Maria, Marco Maria Agostino Rossi, Giacomo Ferrarese, and Stefano Malavasi. "Numerical investigation of parameters affecting energy losses in multi-stage perforated plates." *Journal of Fluids Engineering* 145, no. 9 (2023): 091204. <https://doi.org/10.1115/1.4062406>
- [29] Yu, Yangyang, Junhong Zhang, Jun Wang, and Dan Wang. "Flame propagation behavior of propane–air premixed combustion in a confined space with two perforated plates at different initial pressures." *Energy Science & Engineering* 10, no. 8 (2022): 2940-2953. <https://doi.org/10.1002/ese3.1180>
- [30] Turkeli-Ramadan, Zerrin, Rajnish N. Sharma, and Robert R. Raine. "Investigation of the effects of flame holder on the combustion characteristics of a flat flame micro combustor." In *ASME International Mechanical Engineering Congress and Exposition*, vol. 45226, pp. 295-304. American Society of Mechanical Engineers, 2012. <https://doi.org/10.1115/IMECE2012-88432>
- [31] Managed Pressure Drilling. (2008). Elsevier.
- [32] Bahr, Donald W. "Gas turbine combustion—alternative fuels and emissions." (2010): 116501. <https://doi.org/10.1115/1.4001927>
- [33] Aravind, B., Velamati Ratna Kishore, and Akram Mohammad. "Combustion characteristics of the effect of hydrogen addition on LPG–air mixtures." *International journal of hydrogen energy* 40, no. 46 (2015): 16605-16617. <https://doi.org/10.1016/j.ijhydene.2015.09.099>
- [34] Guo, B. Y., Q. F. Hou, A. B. Yu, L. F. Li, and Jun Guo. "Numerical modelling of the gas flow through perforated plates." *Chemical Engineering Research and Design* 91, no. 3 (2013): 403-408. <https://doi.org/10.1016/j.cherd.2012.10.004>
- [35] Lefebvre, Arthur H., and Dilip R. Ballal. *Gas turbine combustion: alternative fuels and emissions*. CRC press, 2010. <https://doi.org/10.1201/9781420086058>